Particle ID performance of Liquid Argon TPC

J-PARC T32 collaboration

Abstract

This paper describes a study of particle identification performance of liquid Argon TPC (LArTPC) detector using well-defined charged particles (pions, kaons, and protons) with momentum of 800 MeV/c obtained at J-PARC K1.1Br beamline.

We have build a LArTPC detector with fiducial mass of 150 kg, and injected the beam particle

Keywords:

1. Introduction

Refer [1] for hardware/beam line description

2. Data Quality

2.1. Collected Data

Table 1 shows list of the collected data while Oct/2010 Run. 800 MeV/c pion is expected to pass-through the detector as MIP, and have uniform energy deposition to all the TPC channels. So this data set is very useful for calibrating the detector response (See section xxx). 800 MeV/c proton stops after 15 cm of flight distance inside the TPC fiducial volume with relatively large dE/dx. So we use the proton data set for validation of the detector response at high dE/dx region(See section xxx). We have collected three different Kaon data by varying thickness of the degrader. 540, 630, 680 MeV/c are corresponds to the momentum degraded by 2 lead glass, 1 lead glass + 1 lead block, and 1 lead glass, respectively, and such Kaon stops after 10 cm, 50 cm, and 65 cm of flight distance inside TPC fiducial volume.

Figure 1 shows an 2D display of typical event taken with 800 MeV/c electron trigger. Horizontal axis corresponds to TPC channel number and zero means most upper stream strip. Since strip pitch is 1 cm, this is equivalent to distance from beam injection point in cm. Vertical axis corresponds to electron drift time in μs and t=0 means trigger timing. In this TPC, anode and cathode is located at top and bottom of the detector, respectively, t=0 means energy deposition at anode and longer drift time means energy deposition in lower height. With 200 V/cm of electric field, drift velocity is about 0.8 m/ms. So drift of full detector (40 cm) takes 500 μs. Color strength of the plot corresponds to the TPC signal pulse height in ADC counts which is roughly proportional to dE/dx of the track. In this event, triggered electron can be clearly seen center of the detector as an electromagnetic shower while there are two other particles accidentally overlapped with the triggered electron. Track at t=100 μs is considered as a proton which stops after 15 cm of flight distance and has large dE/dx around the stopped point. Track at t=400 μs is considered as a pion which passes-through the detector and has uniform dE/dx over the TPC channels. This event already gives us some idea for how good the particle identification performance of the LArTPC is.

Figure 2 shows a typical $K \rightarrow \mu\nu$ like event. We can clearly identify a kink of the track at 60 cm which is considered as stopped point of Kaon and it decays to

Energy deposition of the track is about MIP at the injection point and gradually increase towards the stopped point at 60 cm.

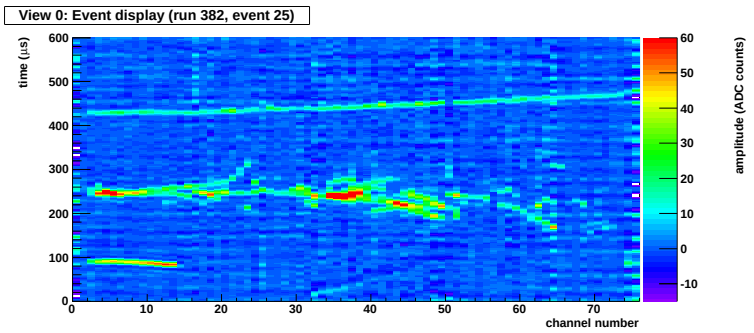

Figure 1: Event display of 800 MeV/c electron triggered event. Accidentally overlapped with a proton and a pion.

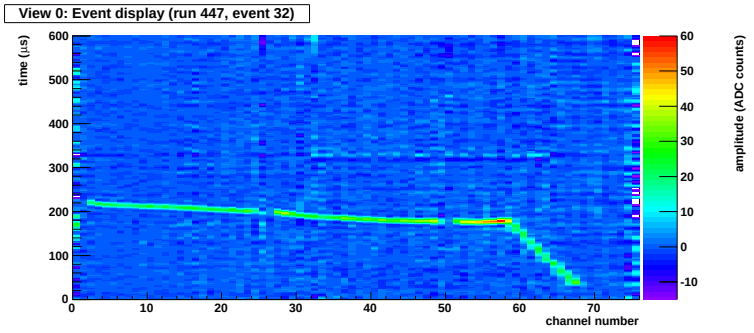

Figure 2: Event display of Kaon 630 MeV/c triggered event

Table 1: List of collected data

Particle	Momentum (MeV/c)	Number of Events
Pion	800	3,000
Proton	800	1,500
Kaon	540 (2LG)	7,000
Kaon	630 (1LG+1LB)	40,000
Kaon	680 (1LB)	35,000
electron	800	2,500
electron	200	10,000
pion	200	10,000

2.2. Beam Quality(Purity)

We have several beam counters to indentify beam particles event by event(see Fig3).Using this when taking data, we can get data of interest selectively.The following describe how to identify beam particles with the typical data including K^+, π +, e^+, p events, which have the momentum adjusted ~800MeV/c.

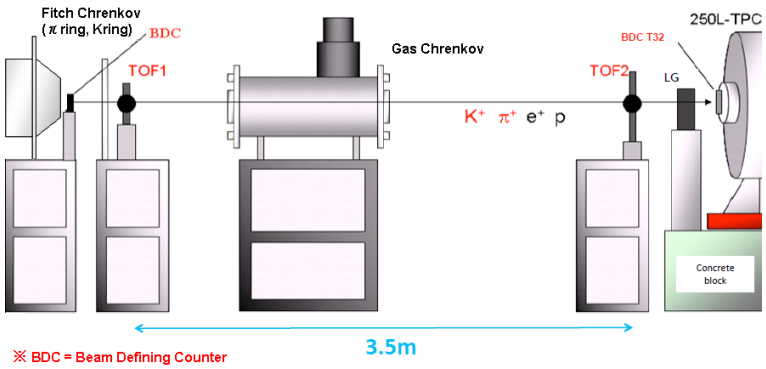

Figure 3: Instruments on K1.1BR Beam Line

Leaded particles to K1.1BR beamline pass the Fitch Cheernkov Counter at first. Fitch Cherenkov Counter can select particles with diffrerences of angle of cherenkov light which they radiate. Fifure4 shows the respose of the Fitch Cherenkov Counter. The horizontal axis shows the total amount of PMT signal where cherenkov light of 800MeV/c π can be detected. The

vertical axis shows that of 800MeV/c K. Signals are distinctly seperated to three cluster and can be categolized as following.

1. FC Signal(π)<1450 & FC Signal(K)>2000
2. FC Signal(π)<1450 & FC Signal(K)<2000
3. FC Signal(π)>1450 & FC Signal(K)<2000

Appearently, particles within the region 1 are K^+ candidates. Particles within region 2 are p candidates because 800MeV/c p is impossible to radiate cherenkov light. Particles within region 3 are π^+ or e^+ candidates because their angle of cherenkov light are almost same level.

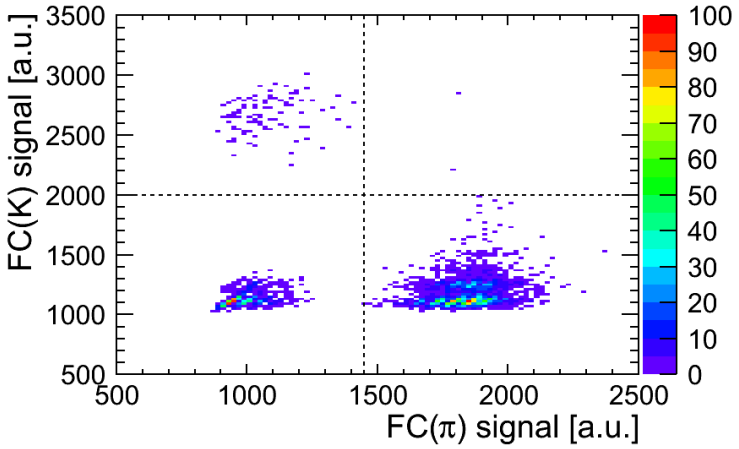

Figure 4: Fitch Cherenkov Counter

Gas Cherenkov Counter can select e^+ from the other particles because only e + can radiate cherenkov light at the refractive index of this gas. Figure5 shows the responce of the Gas Cherenkov Counter. The horizontal axis shows the PMT signal of the Gas Cherenkov Counter. The vertical axis shows the number of events. Fitting the pedestal with gaussian function, the events larger than the value added $\sim 3.5\sigma$ to the mean of the pedestal is

particle	e^+	π^+	K^+	p
Mass(MeV)	0.511	139.57	493.68	938.27
Time of Flight(ns)	11.67	11.84	13.71	17.98

Table 2: Time of flight of eash particle

e^+ candidates.In this case, GC signal is required more than 104.7 to be e^+ candidates.

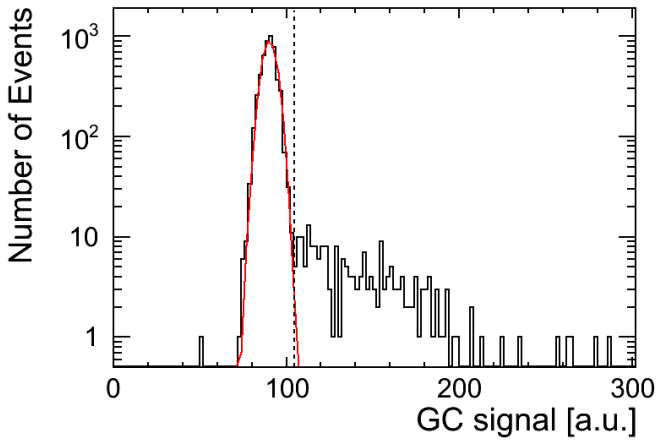

Figure 5: Gas Cherenkov Counter

There are two TOF Counters which has ∼200ps resolution 3.5m apart, and each particle can be selected with the difference of time of flight between them. Following table2 is calcurated time of flight when each 800MeV/c particle passes two conters. As this table shows, $e+$ and π^+ cannot selected because the difference of time of flight is too short for the TOF resolution.

Figure6 shows responce of the TOF Counters. The horizontal axis shows the time of flight between TOF1 and TOF2 Counter. The vertical axis shows the number of events. Signals have clearly divided three structures. From table2, in asending order of time of flight the first structure include e^+ or π^+ candidates, and the second struature include K^+ candidates, and the third structure include p candidates. The cut value to separete the first strucuture and the second structure is $\sim 4.5\sigma$ (in this case, the value is setted

13.15ns), and because the second structure and the third structure is clearly separated, the cut value to select them is setted 16.47ns fully apart from the second structure.

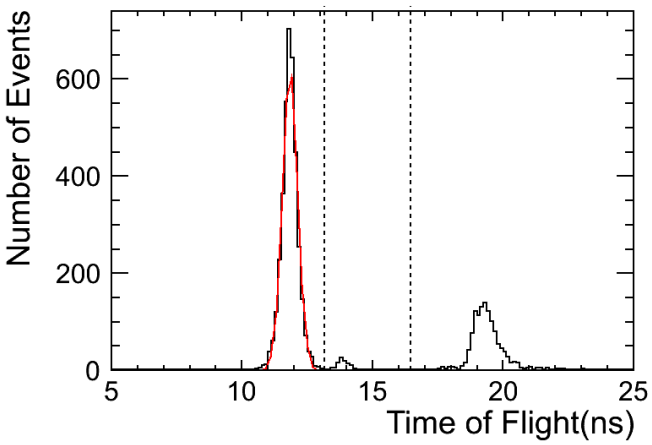

Figure 6: TOF Counter

K^+ can selected very efficiently with Fitch Cherenkov Counter, so we require the condition FC Signal(K) is more than 2000 to get the date of K in taking data. Figure7 shows responce of the TOF Counters before and after above cut. The histgram which filled with black is what is after cut. This figure shows we can get high-purity K^+ samples with this condition.

Particles which satisfy all conditions for the same candidate are identified themselves, and the others are defined 'uncertain' particles. Herewith, we can identify beam particles with high purity before injection to 250L detector. Table2.2 shows the beam components of the data used for analysis.

Run 52,55,59 and 60 are the data required the condition FC Signal(K) is more than 2000 in taking data. As table2.2 shows, these data is almost occupied K^+ events and the ratio is $\sim$98% on average.

2.3. Beam Energy

30GeV proton beam hits to target T1 in Hadron hall. It generates many particles like kaon, pion, muon, electron, and so on. We take the particles that has 800MeV/c momentum from this beam by using D1 magnet.

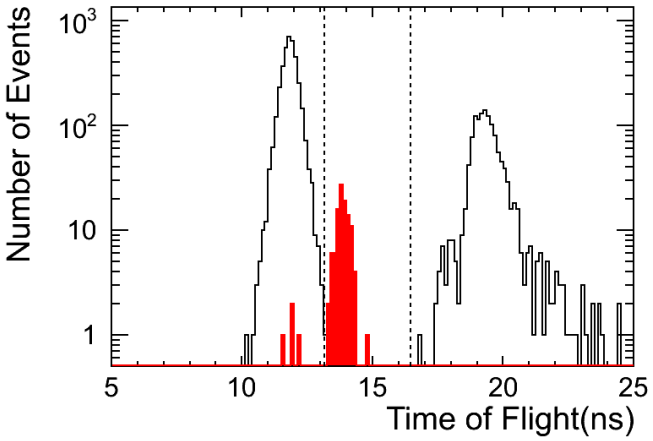

Figure 7: TOF Counter

Run Number	e^+	π^+	K^+	p	*uncertain*	Number of Events
42	68	1617	27	232	5	1949
48	128	1594	78	126	11	1937
49	0	341	0	1146	12	1499
52	0	1	3126	0	76	3203
55	0	6	8386	0	208	8600
59	0	8	5863	0	119	5963
60	0	1	1870	0	40	1911

Table 3: Beam components of data ued for analysis

For this analysis, a beam momentum at BDC after passing through the K1.1Br beam line is required. We estimate a beam momentum using simple MC simulation. Figure 11 shows MC simulation's geometory. This time, beam line is straight and has no electric and magnetic field. MC simulation shoot 800MeV/c kaon and pion as pencil beam.

Figure 12 shows kaon and pion momentum distribution using this MC simulation. Actually, kaon momentum distribution peak is adjusted so that kaon decay point of MC simulation is consistent with data. Section 2.3.1 explains this point. And proton momentum is estimated in other way, using TREK detector TOF information. Section 2.3.2 shows proton momentum distribution.

2.3.1. Kaon energy

We adjust momentum peak of figure ?? and set Kaon beam energy the point that the decay points of Kaon in data and simulation are good agreement. The distribution of decay poins are plotted in Figure8.

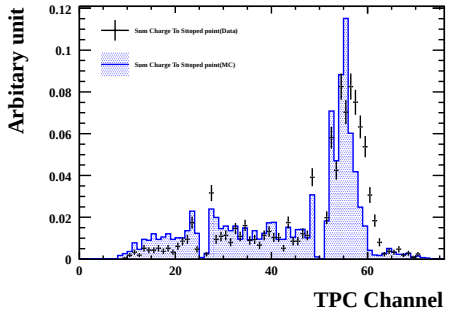

Figure 8: Decay point distribution of Data and MC

2.3.2. Proton energy

Figure9 shows responce of the TOF Counters of selected Proton of Run 49 which includes many proton events. Compared the value of 17.98ns of table2, protons are distributed where is much smaller than this value. This result indicates beam momentum of protons are smaller than ∼800MeV. Futhermore, the dispersion of time of flight of protons is very differnt from the other particles. Based on these fact, the momentum of Proton which implement in simulation is estimated by TOF information. Figure10 shows the estimated

momentum from time of flight between two TOF Counters. Whether the distribution reproduce real momentum well is discussed in section 7.2.

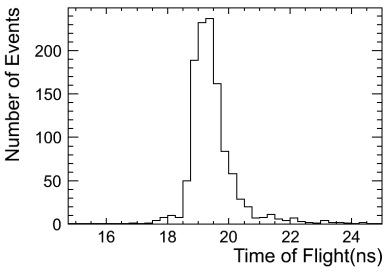

Figure 9: p TOF response

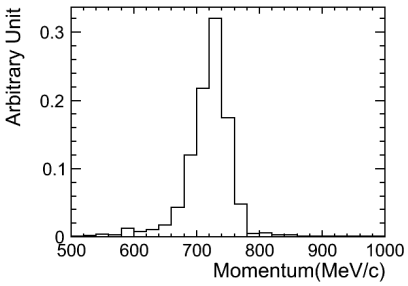

Figure 10: Estimated p momentum

2.3.3. Energy deposition in degrader

Because of having high energy, kaon beam from BDC passes through 250LAr TPC. So that kaon stops in 250LAr TPC, we put degrader, which reduce beam energy, on beam line. In this experiment, we used lead glass and lead block as degrader. We estimate energy deposition in degrader by using MC simulation. Figure 13 shows energy deposition in degrader.

2.4. Beam Position

Before taking data, we measured a beam profile on the front of 250LAr TPC by using plastic scintillation counter. Figure 14 shows beam profile on the front of 250LAr TPC.

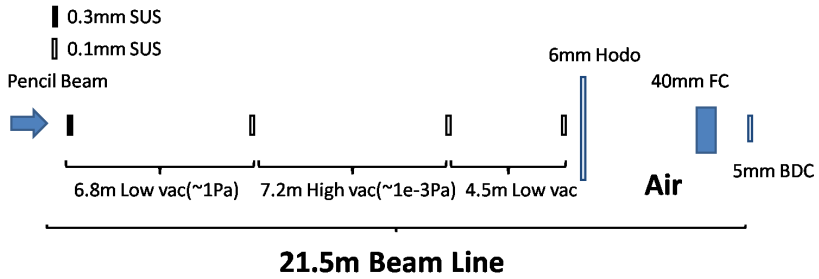

Figure 11: K1.1 Br beamline

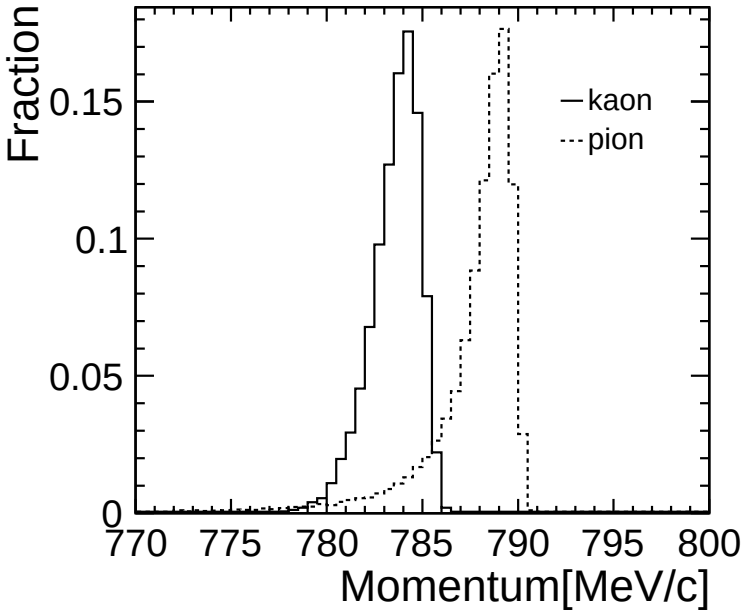

Figure 12: kaon and pion momentum distribution at BDC

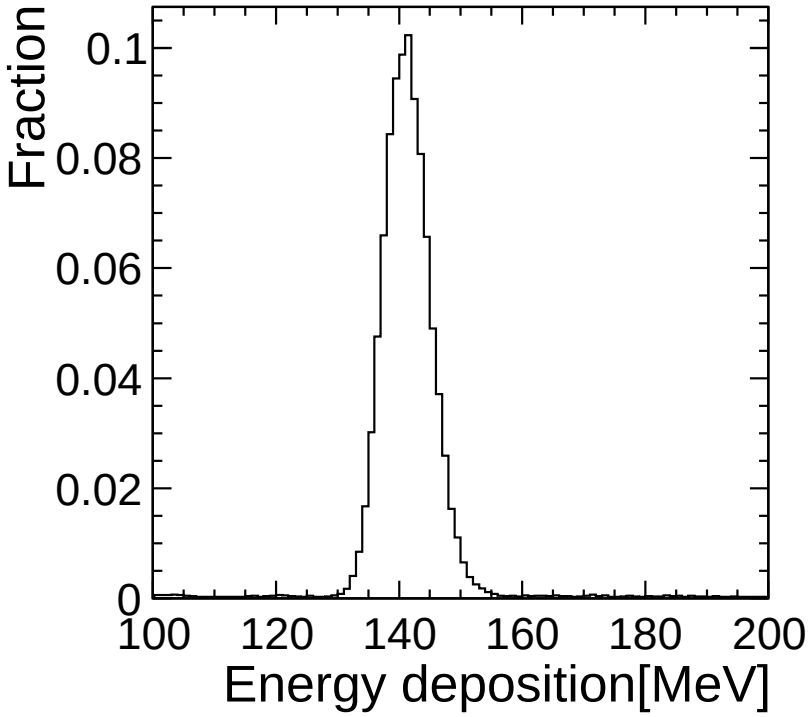

Figure 13: energy deposition in degrader

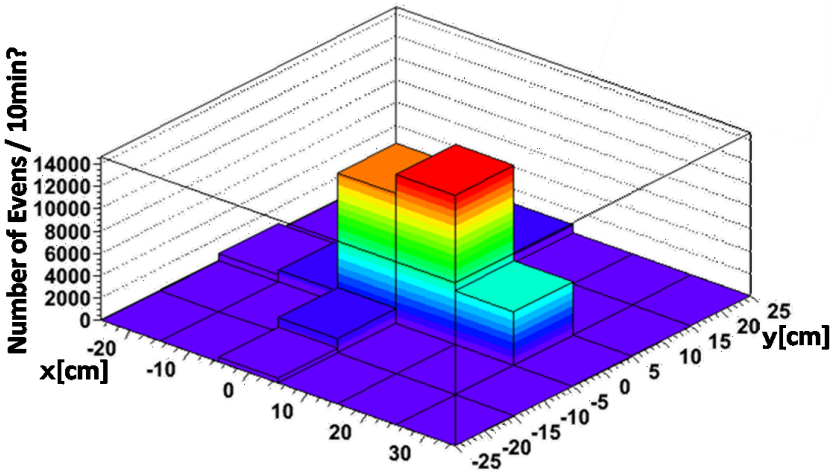

Figure 14: Beam profile on the front of 250LAr TPC

3. Software Framework

Qscan is a general purpose software package for LArTPC analysis(reference) which provides,

- event reconstruction: noise reduction, hit finding, clustering, and tracking...
- event simulation: GEANT VMC with ROOT geometry, ionization electron recombination, drift, digitization...
- event visualization: display raw data waveform and reconstructed quantities

4. Event Reconstruction

4.1. Noise Reduction

Figure 16 shows raw waveform of the TPC signal before applying any noise reduction. Two waveforms shown in this plot are channel 13 and 37 in Figure 1 which are roughly proton stopped point and electron shower maximum point, respectively. Signal-to-noise ratio for this particular case is poor and pion signal which is supposed to be t=400 μs is almost hidden by the noise. While time width of TPC signal is few μs which is determined by drift time between anode and anode-grid, dominant noise component looks higher frequency. To reduce such noises, we have applied FFT (Fast Flourier Transformation) filter to cut the high frequency component. Figure **??** shows amplitude as a function of frequency for the same event. This clearly shows dominant noise component with $>$ 200 kHz has good separation with signal component ($<$ 100 kHz). Figure 17 shows the waveform after removing high frequency ($>$ 80 kHz) component by the FFT filter. Signal-to-noise ratio is dramatically improved. On the other hand, we expect certain bias to the signal charge measurement by this filter, and it will be discussed in Section x.

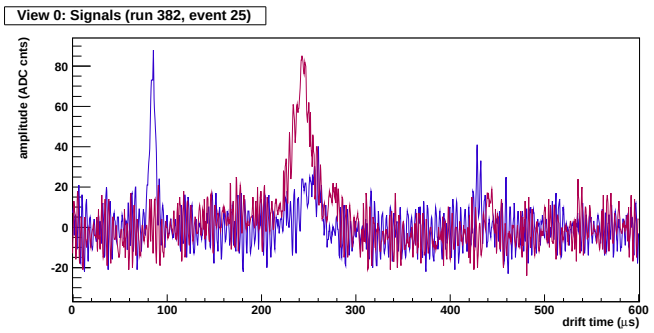

Figure 15: TPC raw signal waveform for "Textbook" event channel 13 and 37.

4.2. Hit Finding/Clustering

After noise reduction we find signal hits and create clusters associated to single tracks. Hit is defined as bump over given threshold in a channel. After finding all hits in an event, we construct cluster by merging adjacent hits. The example of hit finding and clustering is shown in Fig 18, which indicates

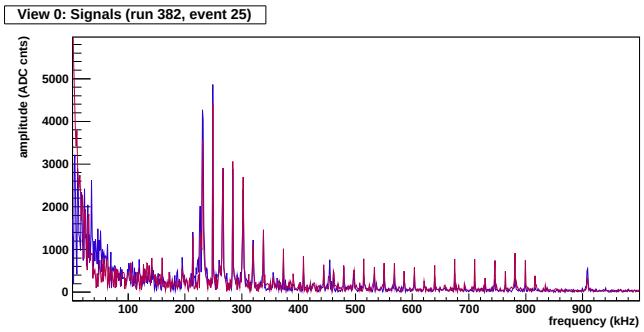

Figure 16: FFT frequency amplitude distribution

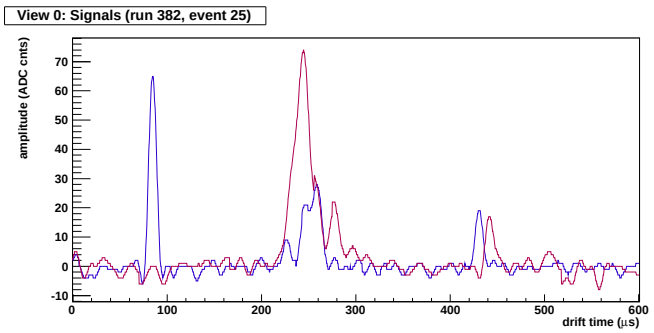

Figure 17: TPC signal waveform after cutting the frequency $>$ 80 kHz.

reasonable hit and cluster findings. Threshold of hit finding is determined to keep enough signal hit finding efficiency from simulation while keeping adequately small number of noise hits from real data.

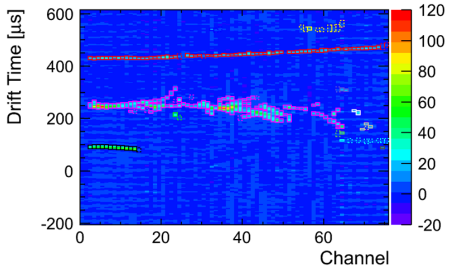

Figure 18: Example of hit finding and clustering. A colored box corresponds to a hit and colors represent different clusters.

- Plot: Finding efficiency vs threshold (Naganoma): TBU
- Plot: Through-going pion data Q vs pion (Tanaka)

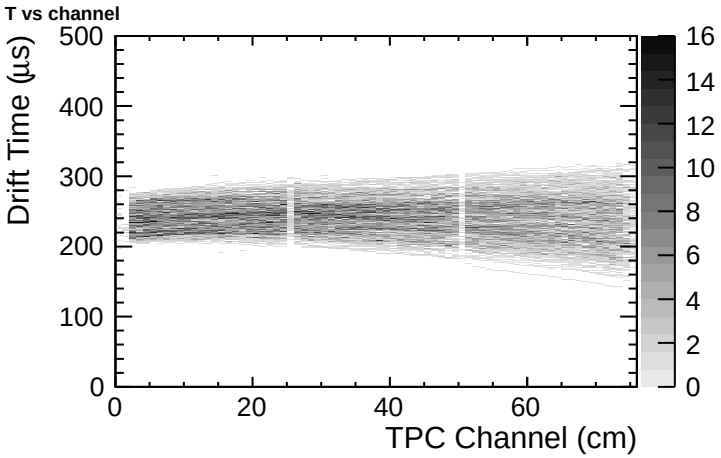

Figure 19: 800 MeV/c pion sample

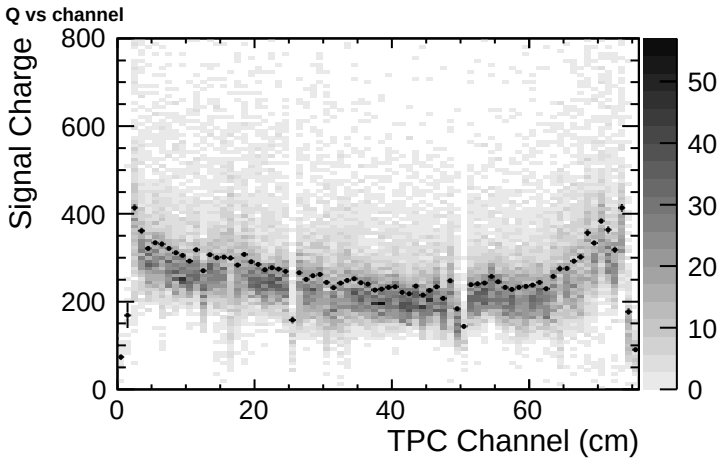

Figure 20: 800 MeV/c pion average hit charge

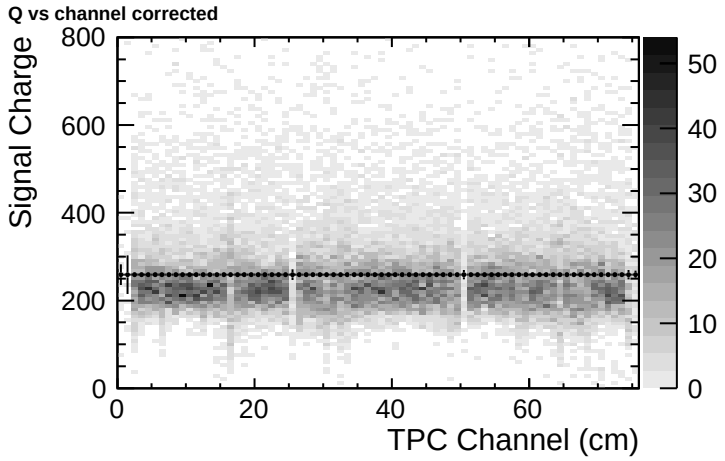

Figure 21: 800 MeV/c pion average hit charge after calibration

4.3. Stopped Point Finding

4.3.1. Proton

Figure22 shows typical event of proton. Proton has simple structure of events because proton doesn't decay any particles. Therefore, it is easy to define stopped point. First, protons are selected by the information of beam counters. Then, proton events are applied following simple selections.

1. The time of the hit of the minimum channel number in the cluster is between 354.8ns∼504.8ns(this time window is signal region).

2. The minimum channel number of hits in the cluster is below 2.

3. The maximum channel number of hits in the cluster is below 60.

4. The total hit number in the cluster is 5 or more.

5. The number of hits which are in the same channel is only one.

We define the events which the number of clusters in the event which passed above selections is only one as good proton events. For protons was chosen in a such way, we define the hit which has the maximum channel number as stopped point. It should noted that stopped point include fake hit in a proportion because of the influence of cross talk as described in section 6.6.

4.4. Stopped Kaon

Hough transform was invented for machine analysis of bubble chamber photographs by Paul.V.C.Hough.[6] We detect straight lines using hough method , and find Kaon stopped point from the intersection of straight lines. Figure 23 shows hit map like a Kaon track. One point in the X-Y space can be transformed into sinusoidal curve in the ρ-θ space.Figure 24 shows sinusoidal curves in all points. And, we detect the straight line associated with the largest number of points by choosing the most dense point in ρ-θ space. Next , the sinusoidal curves of the hits associated with frist straight line are removed from figure 24. Figure 25 shows sinusoidal curves after the

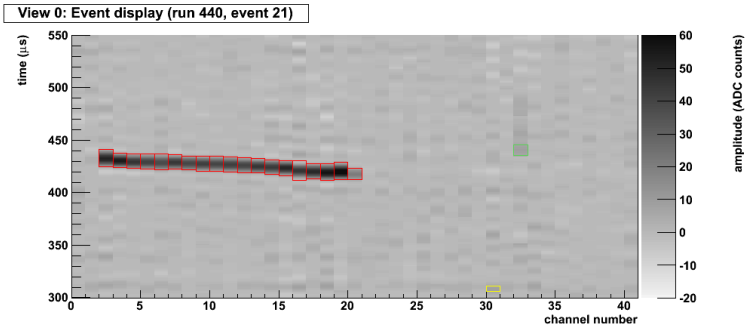

Figure 22: Typical Event Display of Proton

hits associated with frist straight line removed. We detect second straight line using the same procedure.This procedure is repeated until there are less than three points.Figure 26 shows the two straight lines detected by hough transform mehotd.
Kaon stopped point in the liquid argon detecor defined as charge maximum point around the intersection of some lines.

4.4.1. Chi2 method

χ^2 method is the algorithm that search the point of rapidly increasing fit'χ^2 and the point defined as the stopped point. Because the charged particle coming from upsteam of beam line , track reconstruction is started from minimum channel to the maximum channel of the cluster.
Figure 27 shows hit map like a Kaon track. We start fitting with straight line from minimum channel to maximum channel.Figure 28 shows range vs fit'χ^2 distribution. As it can be noiced for figure 28, χ^2 is increased rapidly if the straight line is strayed out. Then , we search the strayed point from the straight line by setting reasonable threhold and draw from minimum channel to the strayed point. This procedure is done from maximum channel to minimum channel in the same way. And we draw from maximum channel to the strayed point. Kaon stopped point in the liquid argon detecor defined as charge maximum point around the intersection of two lines.

4.4.2. BS method

In the χ^2 method , we can't detect Kaon stopped point in the case of backward decay. Then , we detect Kaon stopped point using BS method.
BS method is concept that the Kaon stopped point defined as lightmost

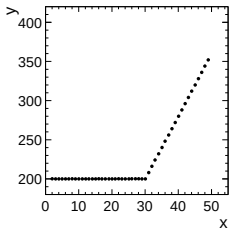

Figure 23: Hit map like a Kaon track

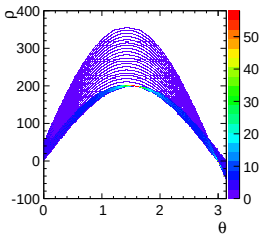

Figure 24: sinusoidal curves getting form all hough transformed points of Figure 23

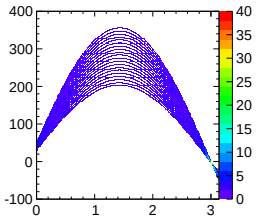

Figure 25: sinusoidal curves removed the points associated with first straight line from figure 24

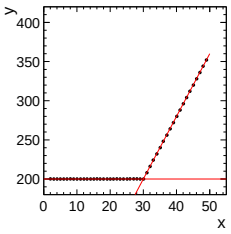

Figure 26: Two lines detected with hough transform method

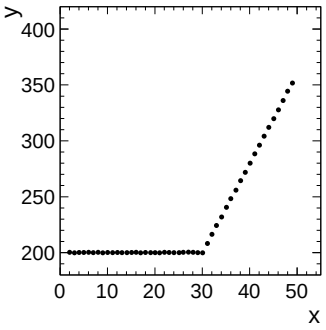

Figure 27: hit map like a Kaon track

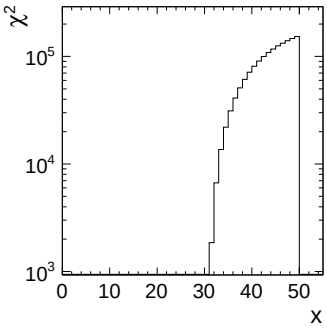

Figure 28: range vs χ^2 distribution

channel in the case of backward decay. we descript below how the track defined as backward decay. N_1 is defined as Number of cluster hits found by the clustering. Stopped point finding is started from minimum channel.

We search for the closet timing hit in next channel from current channel hit. Then , we repeat this procedure until maximum channel and count the number of selected hit information(N_2). In the case of backward decay , N_1 is larger than $N2$. So , we set reasonable threhold of the difference between N_1 and $N2$, and if the $N_1 > N_2$ is over the threshold , the track is defined as backward decay. In the case of backward decay , we defined charge maximum point around the maximum channel as the stopped point.

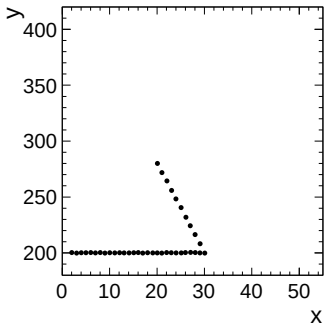

Figure 29: hit map like a Kaon track

5. Liquid Argon Purity

Attenuation of the drift electron depends on purity of LAr since electronegative impurities capture it [5]. Thus we need to apply correction to TPC signal charge depends on the drift time. We use cosmic ray sample triggered by inner PMT at off-beam timing for measuring the LAr purity, and use this to correct the beam data. Figure 30 shows an event display of typical cosmic muon event across TPC channels. The attenuation of readout charge depending on drift time is clearly seen in the right plot. Readout charge in an event cannot be fitted by exponential because energy deposition follows Landau distribution and charge readout is affected by electric field distortion which is described latter in section **??**.

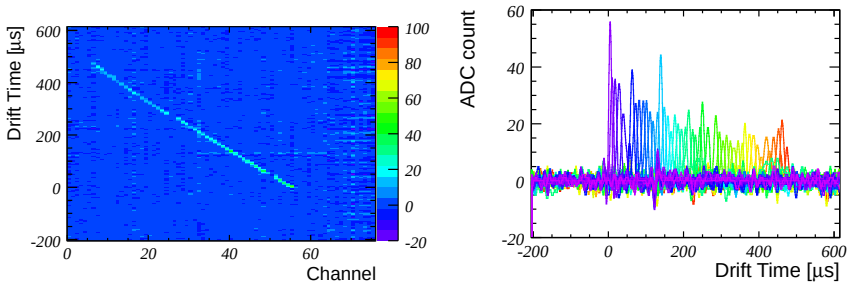

Figure 30: Left: Typical cosmic muon event across TPC channels. Right: Charge deposit as a function of drift time. Colors correspond to different TPC channels.

We select cosmic ray event with more than 20 TPC channels which corresponds to zenith angle of more than 27° and consistent with straight line by χ^2 fit. Readout charge is corrected for field distortion and projected to beam direction to correct injection angle. We fit readout charge by Landau function in each drift time bin to estimate average charge deposit. Figure 31 shows example of the average readout charge as a function of drift time which is fitted by exponential to obtain drift electron lifetime. Realistic Monte Carlo simulation shows about 13% (TBU) smaller lifetime estimation due to noise, field distortion, and FFT effects. We correct output lifetime from these effects. Figure 32 shows an drift electron lifetime as a function of duration after initial LAr filling. Drift electron lifetime was 600 μs at 60 hours, and 400 μs after 150 hours. The degradation is possibly due to impurity from micro

leak or out-gassing penetrating faster than purification by gas recirculation. But we kept enough drift electron lifetime during data taking period.

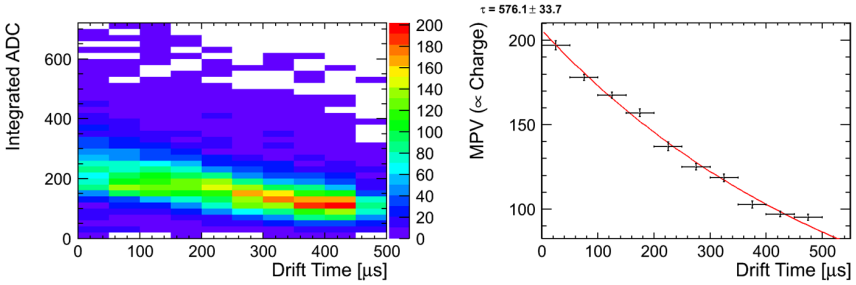

Figure 31: TBU. Left: Readout charge as a function of drift time. Readout charge in each drift time bin is fitted by landau function. Right: Average charge readout as a function of drift time which is fitted by exponential to estimate drift electron lifetime.

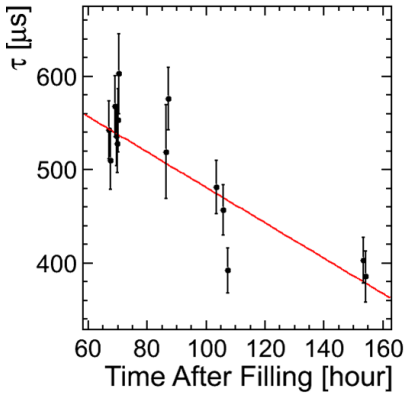

Figure 32: TBU. Drift electron lifetime as a function of duration after initial LAr filling. The lifetime is used to correct the beam data.

6. Event Simulation

6.1. Geant3, recombination, drift velocity

We use GEANT3 for simulating energy deposition of initial beam particles and secondary particles to LArTPC detector and beamline counters.

we set the maximum step of Geant to 0.5 mm which is enough smaller than the readout pitch of 1 cm. It means charge deposition in one strip is typically simulated with 20 GEANT steps.

We set energy cut-off for soft electron/photon emission to 10 keV which is minimum possible energy can be set in GEANT3. This cut-off is very important for ionization electron recombination.

Recombination of electron and Argon ion depends on the electric field and dE/dx. We use a measurement in Ref.[3].

$$Q = A\frac{Q_0}{1 + kdE/dx}, A = 0.800, k = 0.486 \quad (1)$$

Velocity of the drift electron depends on the liquid Argon temperature and the electric field. We use a measurement in Ref [4].

- Plot: Geant Geometry, typical track (Tanaka)
- Plot: recombination factor, drift velocity (Tanaka)

6.2. Electric Field

Electric field of the TPC field cage We have calculated the electric field using a 2D FEM (Finite Element Method) package [**?**].

This field map is used for simulating electron drift.

6.3. Drift Electron Diffusion

- Plot: drift simulation (Tanaka)

6.4. Preamp Gain Calibration

- Preamp gain vs channel number (Naito)

6.5. FFT Noise

Adding realistic noise to MC simulation is very important. In this section, we will introduce how to make realistic noise and implement to MC.

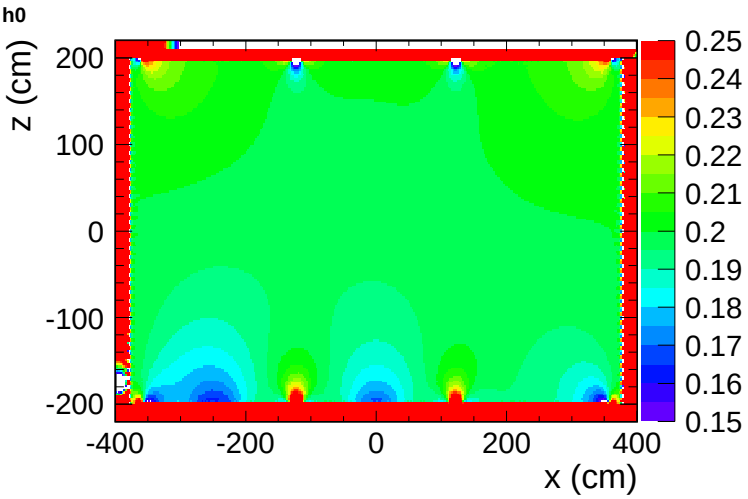

Figure 33: Electric field map obtained from 2D FEM calculation

6.5.1. Noise information of Real DATA

As a first step, we checked distributon of frequency from real data using FFT(Fast Fourier Transform)(see Fig34). Next, We got distribution of amplitude value channel by channel and frequency by frequency. Fig34 shows an example. In this event, amplitude is 200 about 400 [kHz] in 10 channel. After repeating this procedure, we could obtain histograms of amplitude value channel by channel, frequency by frequency(35). We used these histograms to reproduce realisitic noise. Details are described in the next section

6.5.2. Making FFT noise

The procedure of making FFT noise is below:

1. Get amplitude from the histograms of amplitude at random.
2. Perform Inverse FFT

After performing inverse FFT, there is random noise (Fig36)which have the same distribution of frequency as real data. Real DATA have coherent noise but random noise don't have coherent components, therefore adding coherent components is necessary to reproduce realistic noise.

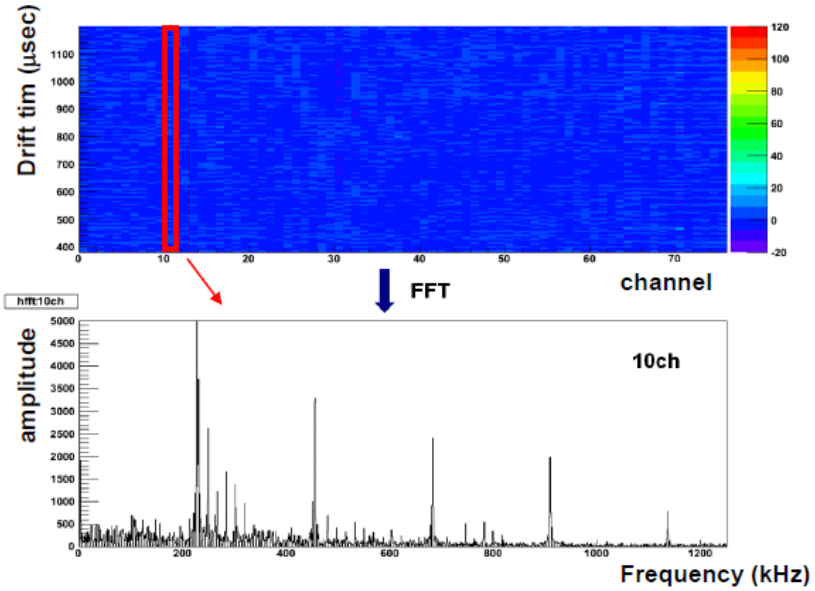

Figure 34: example distribution of frequency:10ch

3. Select random noise 0 and 31 and 63ch
4. Insert random noise 0 ch to 1-30ch, 31ch to 32-62ch, 63ch to 64-75ch
5. Scaling each channel

Real DATA look having coherent noise board by board(We used 3 readout board in T32 experiment). We chosen 3 random noise(0ch,31ch,63ch) in this reason. After that, each channel needs to be corrected as each noise scale. Fig37 shows coherent noise after scaling as Fig38. Vertical axis of Fig38 is RMS of FADC, it stands for noise level.

6.Mixing Random noise and Coherent noise.

Finaly, We mixed Random noise and coherent noise as

$$RealisiticNoise = RandomNoise + CoherentNoise * 0.5 \quad (2)$$

- Plot: simulated event (Nagasaka)

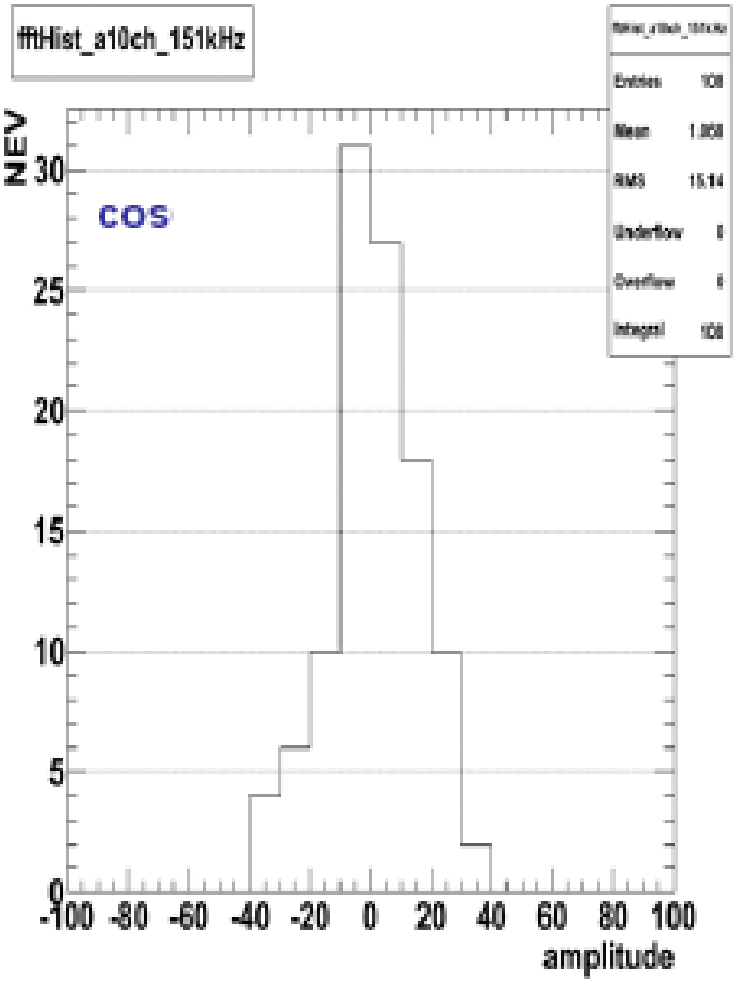

Figure 35: An example of distribution of amplitude

6.6. Cross Talk

The distance between anode channels is very short, so the influence of mutual capacitance become large and this capacitive coupling induce cross talk noise. This effect notably appears the channel where the differnce of the charge between adjacents channels is large, such as the channel around stopped point of proton. Figure?? shows the signal wave form of stopped channel and the front channel of typical proton event. The signal wave form of stopped channel is differencial form of the one of the front channel. This

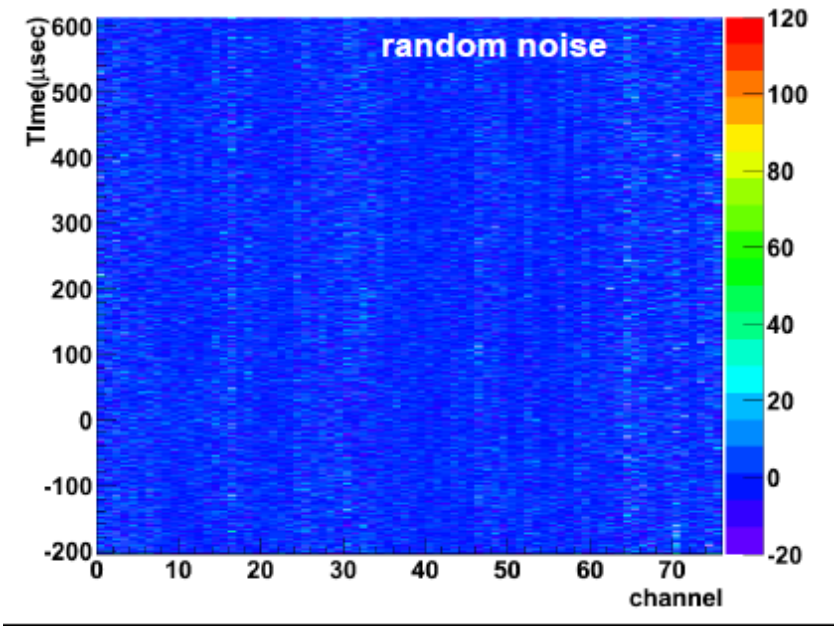

Figure 36: Random noise

shape is appeared at channel number 1 which cannot enter drifted ionization electron in electric power lines. These facts show the exisitence of cross talk. Then, we implement this crosstalk phenomenon in Monte Carlo Simulation by adding bipolar shape of the signal gaussian shape at adjacent channels. The area of the mountain of cross talk bipolar shape is 10.5% of the area of signal gaussian at each adjacent channel. The value of 10.5% is determined by comparing the distribuntion of integrated ADC at stopped channel between DATA and MC. Figure**??** shows integrated ADC distribution of stopped channel. Black is DATA and blue is simulation with cross talk red is simulation without cross talk. As this figure shows, DATA and MC with cross talk is good agreement, and the value of 10.5% is reasonable.

- Plot: signal waveform (proton stopped point + 1) (A. Okamoto)
- Plot: simulated event with and without cross talk (A. Okamoto)

6.7. Signal and Noise Scale Tuning

- Plot: Landau distribution after the tuning (Tanaka)

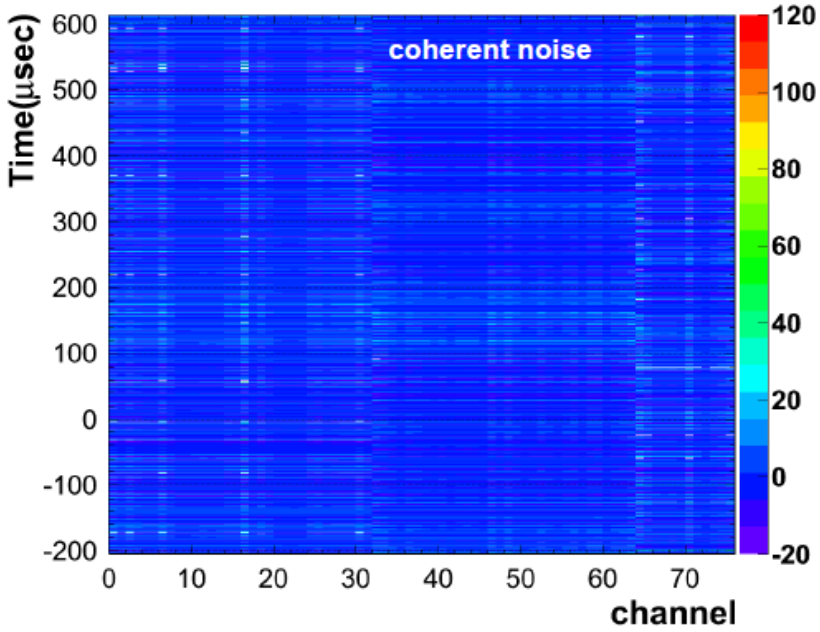

Figure 37: Coherent noise

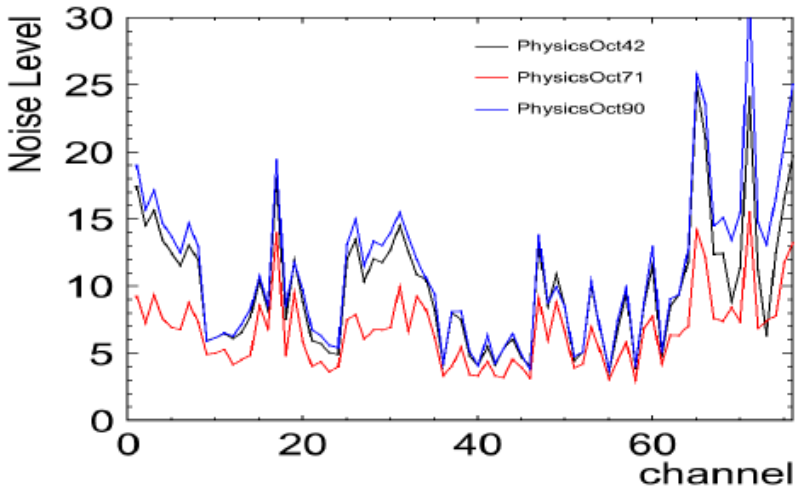

Figure 38: Noise level

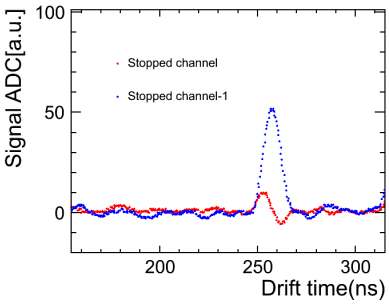

Figure 39: Signal wave form of stopped channel and the front channel

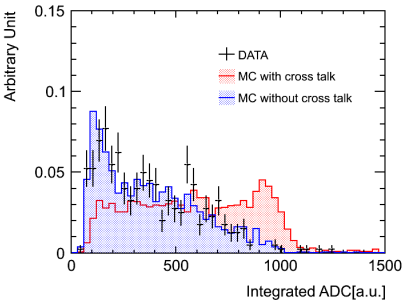

Figure 40: Integrated ADC distribution of stopped channel

7. Data- MC Comparison

7.1. Through-going Pion

- Plot: Data-MC comparison (Tanaka)

7.2. Stopped Proton

When we indicate the validity of charge response in high dE/dx region, proton is good sample due to its simple event structure. At the same time, we verificate the recombination factor by proton in this analysis because proton has wide dE/dx range, and this is meaningless if the charge response of MC doesn't agree with that of DATA. Therefore proton is very impotant in terms of comprehension of charge response.
Figure**??** shows the comparison of the distribution of Hit Charge, Hit Sigma, Stopped Channel and Cluster Charge between DATA and MC. Hit Charge shows the distribution of the integral which fit signal wave form with gaussian. Hit Sigma shows the distribution of all the dispersion which fit signal wave form with gaussian. Cluster Charge shows the sum of the Hit integral of the cluster which is selected as good proton event. All four distribution of MC reproduce DATA well. Especially, the agreement of stopped channel distribution indicates the success of the momentum estimation by TOF infomation because where proton stopped depends on the initial momentum.

Figure42 shows the integrated ADC distribution of each channel from stopped channel. The MC distribution of the channels after stopped channel are good agereements with DATA.
The left of figure43 shows the mean of the above distribution of each channel. The right of figure43 shows the ratios of DATA/MC. The ratios are surpressed within 94%$\sim$104%. From this result, we succeed in reproducing the charge response of DATA in high and wide dE/dx region.

7.3. Stopped Kaon

7.4. Recombination Factor

Electron-ion recombination depends on the electric field and stopping power dE/dx. We have studied this factor using tagged proton beam. Recombination factor measurement using proton beam is relatively easy because of stability of proton. This is why we used proton beam for this study as a first step.
Expression for recombination can be derived

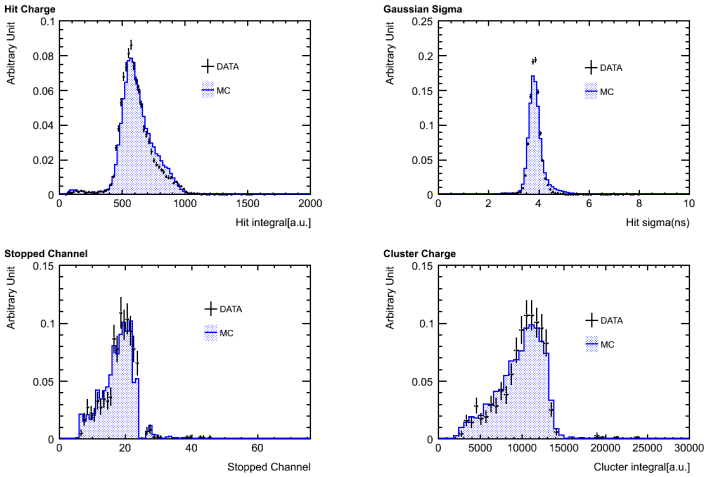

Figure 41: DATA-MC comparison of Hit Charge, Hit Sigma, Stopped Channel, Cluster Charge

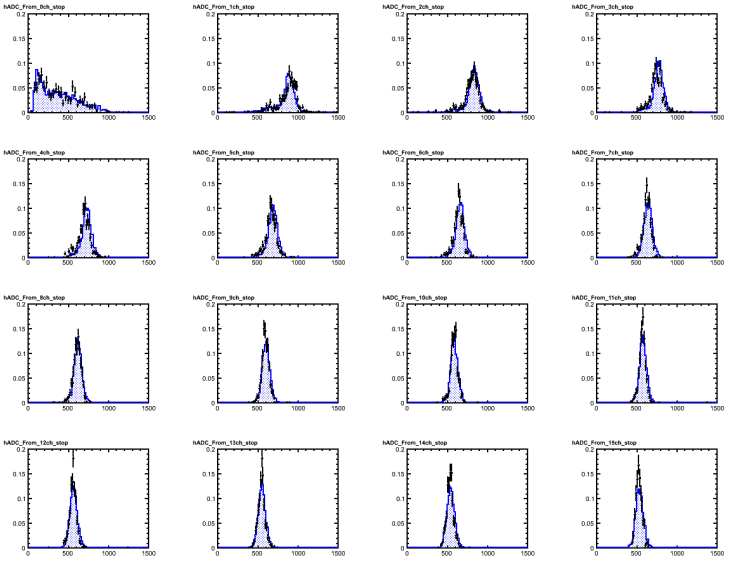

Figure 42: Integrared ADC distribution of each channel from stopped channel

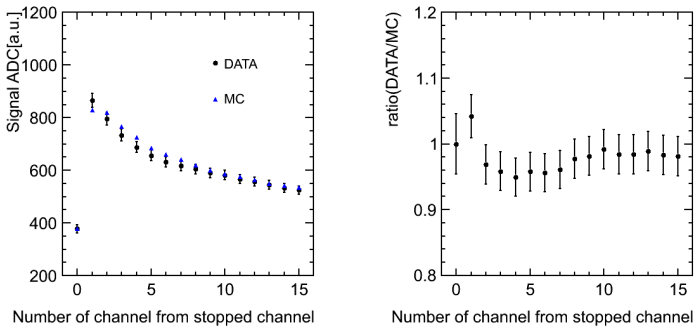

Figure 43: DATA-MC comparison of the mean of Integrated ADC distribution

$$Q = A\frac{Q_0}{1 + (k/E) \times (dE/dx) \times (1/\rho)} \tag{3}$$

where Q_0 is initial ionization charge, E is electric field, dE/dx is energy deposit per distance, ρ is density of liquid Argon, A and k are fit parameters. This formula can be rearranged like below:

$$\frac{Q_0}{Q} = \frac{1}{A} + \frac{(k/E)(dE/dx)(1/\rho)}{A} \tag{4}$$

The ratio of Q_0/Q depends on stopping power dE/dx, so we determined fit parameter A and k using proton data and Monte Carlo simulation. In this analysis, we need Q, Q_0 and dE/dx channel by channel. First, Electric Field E is fixed at 0.196 [kV/cm]. Second, Q is integrated charge in an anode readout channel. we can get this value from Real DATA. Third, Q_0 is integrated charge without recombination factor in an anode readout channel. This value can be obtained using Qscan. And then, dE/dx per an anode channel is determined with truth information of Qscan MC. Fig44, 45, 46 shows Q, Q_0, $dEdx$ from stopped channel -1 to stopped channel -14. In many case, integrated charge in stopped channel are composed of cross talk. This is the reason why we don't use information from stopped channel in this analysis.

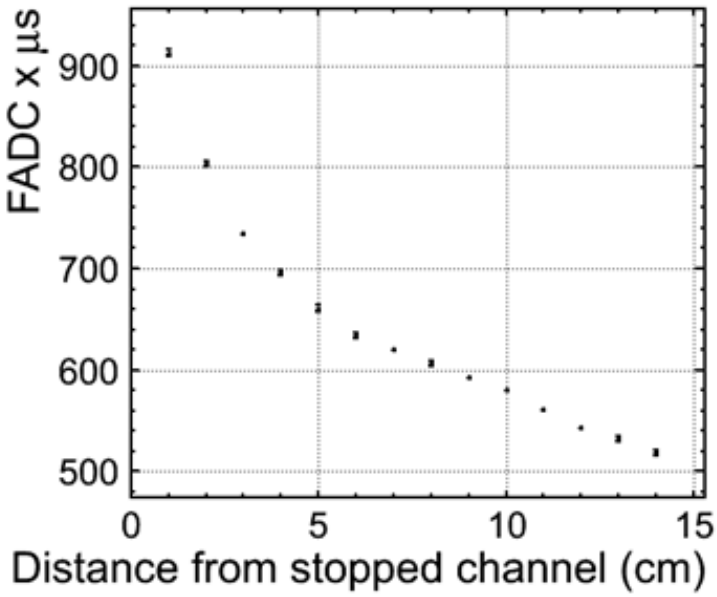

Figure 44: DATA:Integrated Flash ADC counts from stopped channel -1

The result of this study is shown in Fig47. Vertical axis is Q_0/Q, and horizontal axis is dE/dx in this figure, this plot is fitted by Birk's low. As a result, we got fitting parameter

$$\begin{aligned} A = & \quad 0.782 \pm 0.009 \\ k = & \quad 0.0467 \pm 0.0009 [kV(g/cm^2)/cm/MeV] \end{aligned} \tag{5}$$

We checked Birk's low in the range 4 $[MeV/(g/cm^2)] \leqq dE/dx \leqq 12$ $[MeV/cm^2]$ and the result is consistent with ICARUS experiment's one in – sigma.

7.5. Stopped Kaon

In this section , we compare some quantities of data and MC simulation that K stop in the liquid argon detector and can detect stopped point. Figure 48 shows Data and MC comprison for signal hit charge , sigmal width , cluster charge and primary paricle charge distribution. Data of signal charge and signal width are consistnt with MC one in error by less than two % and data

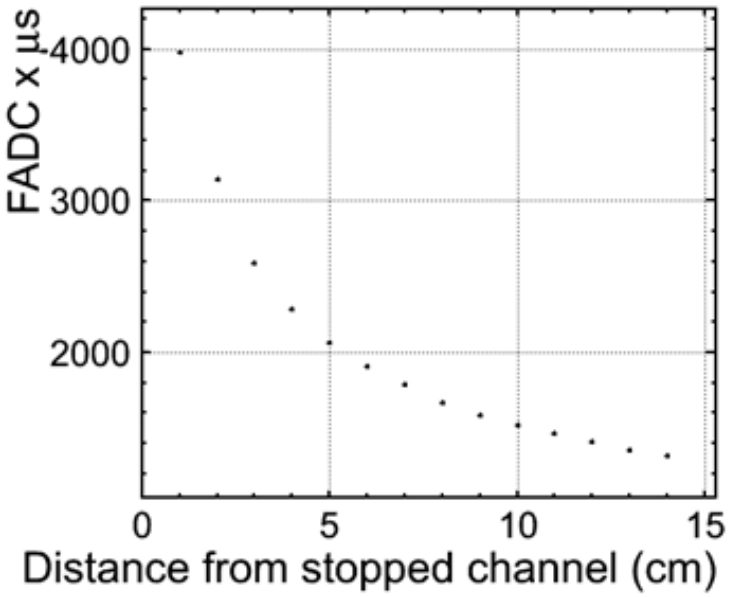

Figure 45: MC without recombination:Integrated Flash ADC counts from stopped channel -1

of cluster charge and parimary charge are consistent with MC one in error by less than five %.

Figure 7.5 shows signal hit charge distribution of restricted channel 27. As it can be noiced for figure 7.5 , signal charge have two peaks at 300 and 500 dQ/dx. Because two peaks has correlation of ΔTOF , there is some possibility of not passig in the center of the detector. So , we use only the event that signal charge of restricted channel 27 is less than 350. Figure 50 shows signal hit charge distribution in different distance from the stopped point.

As it can be noticed for figure 50 , data plot is consistent with MC one. Figure 52 shows data/MC ratio of signal hit charge distribution in different distance from the stopped point. Data of signal charge in dirfferent distance from stoppd point are consistnt with MC one in error by less than five %

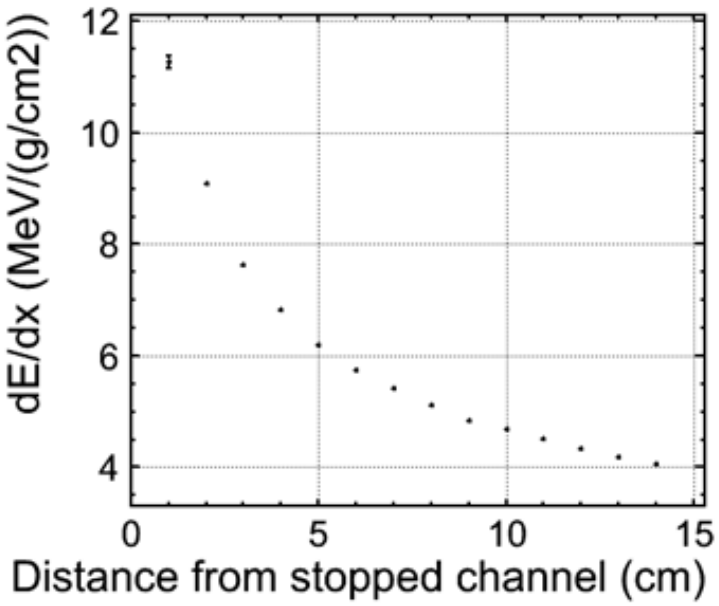

Figure 46: dE/dx from stopped channel -1

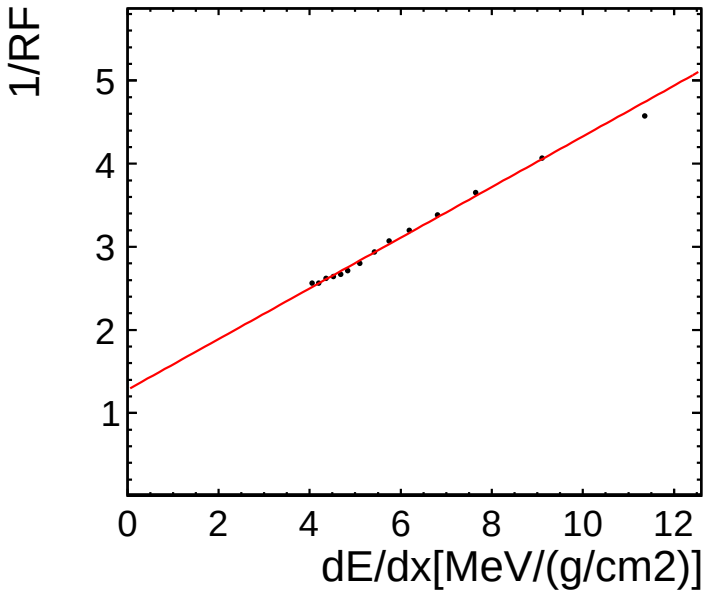

Figure 47: 1/RF VS dE/dx: fitted by Birk's low

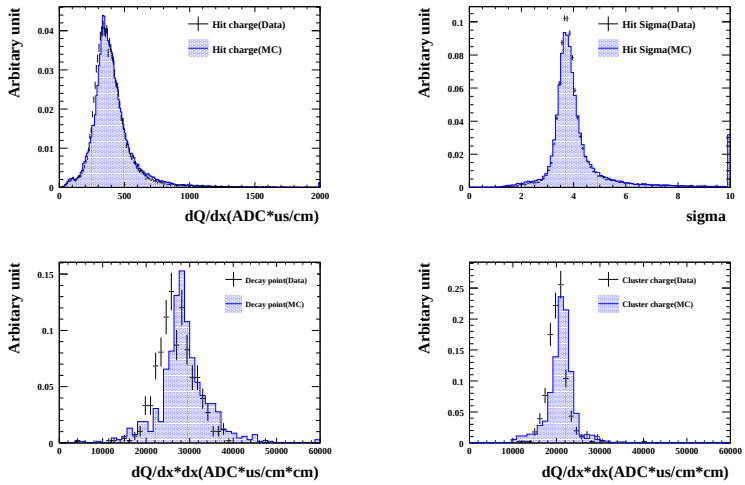

Figure 48: Data-MC comparison for hit charge, hit sigma, cluster charge, primary particle charge

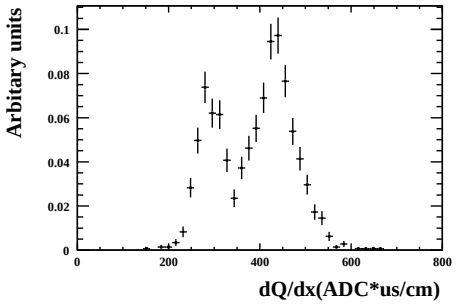

Figure 49: Hit charge in channel 27

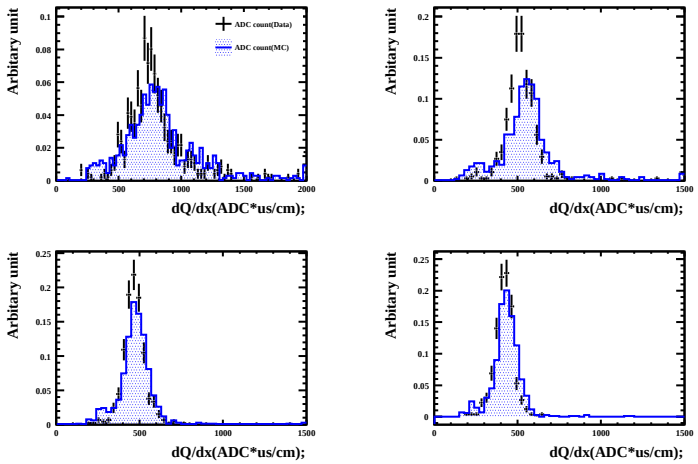

Figure 50: Data-MC comparison for hit charge distribution in different distance from the stopped point(top left:decay point,top light:decay point-5cm,bottom left:decay point-10cm,decay point-15cm)

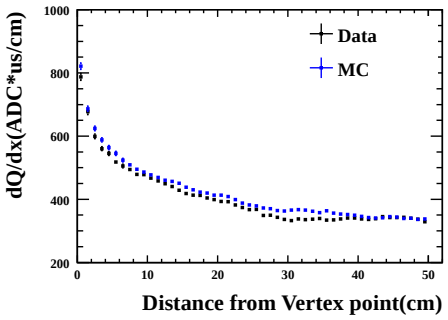

Figure 51: Data-MC comparison for hit charge distribution in different distance from the stopped point

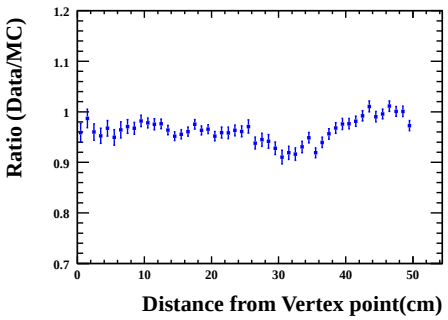

Figure 52: Data/MC ratio for hit charge distribution in different distance from the stopped point

8. Summary

References

[1] O. Araoka *et al.*, J. Phys. Conf. Ser. **308**, 012008 (2011) [arXiv:1105.5818 [physics.ins-det]].

[2] S. Mihara [MEG Collaboration], Nucl. Instrum. Meth. A **518**, 45 (2004).

[3] S. Amoruso *et al.* [ICARUS Collaboration], Nucl. Instrum. Meth. A **523**, 275 (2004).

[4] S. Amoruso, M. Antonello, P. Aprili, F. Arneodo, A. Badertscher, B. Baibusinov, M. Baldo-Ceolin and G. Battistoni *et al.*, Nucl. Instrum. Meth. A **516**, 68 (2004).

[5] A. Bettini *et al.*, Nucl. Instrum. Meth. A **305**, 177 (1991).

[6] P.V.C Hough 'Method and means for recognizing complex patterns',United States Patent Office 3069654(1962)